

Induced anisotropy and phase transformation in metallic glasses by pulsed-excimer-laser irradiation

M. Sorescu and E. T. Knobbe

Oklahoma State University, Department of Chemistry, Stillwater, Oklahoma 74078-0447

(Received 4 August 1993)

Ferromagnetic amorphous ribbons (Metglas 2605 CO, Metglas 2605 SM, Metglas 2826 MB, and Metglas 2605-S3A) were exposed isochronally to pulsed-excimer-laser irradiation ($\lambda=308$ nm, $\tau=26$ ns) by employing various repetition rates and pulse energies. The effects of laser treatment were studied by transmission Mössbauer spectroscopy and scanning electron microscopy. Complementary information was obtained using conversion electron Mössbauer spectroscopy and energy-dispersive x-ray analysis. At moderate values of the repetition rate and pulse energy, controlled magnetic anisotropy could be induced in the higher magnetostriction samples without the onset of crystallization. Similarly, a random distribution of magnetic-moment directions was obtained in the lower magnetostriction samples. The laser-induced changes in the magnetic anisotropy were correlated to the presence of molten zones subsequently quenched and of correspondingly induced mechanical stresses. Analysis of the magnetic texture of the irradiated surfaces supported the model of closure domain structure. At higher values of the repetition rate and pulse energy, the nature of the observed phase transformation could be elucidated by a combination of complementary methods. The effect of excimer-laser-induced crystallization in metallic glasses was evidenced and explained considering characteristics of high-fluence laser irradiation. Through a suitable selection of irradiation parameters, the effects of induced anisotropy and partial crystallization can be used following the laser treatment proposed for tailoring the magnetic properties of metallic glasses with regard to specific applications.

I. INTRODUCTION

Soft ferromagnetism, mechanical resistance, and magnetic coupling in metallic glasses can be modified by annealing in the presence of magnetic fields and/or mechanical stresses.^{1,2} Alternatively, cw laser annealing can be used to promote structural relaxation or crystallization in amorphous ferromagnetic ribbons.³ Improved thermal stability and different crystallization kinetics have been shown to characterize the effect of ultrashort pulse laser annealing in several binary amorphous alloys.⁴ In addition, different stress distributions can be obtained in metallic glasses with negative magnetostriction, as a result of inhomogeneous heat flows produced by local laser annealing.⁵

To date, pulsed excimer lasers have been extensively used to irradiate semiconductor materials,⁶ but they are expected to play an important role in laser processing of amorphous metals as well. Pulsed excimer lasers offer improved beam homogeneity, and better pulse-to-pulse shape and energy-density reproducibility (compared to solid-state lasers), and the possibility of employing high repetition rates even at high pulse energies. Recently, changes in the magnetic anisotropy of Fe-B amorphous alloys have been induced without the onset of crystallization through the use of multipulse-excimer-laser irradiation.⁷⁻¹¹

In the present work, samples of metallic glasses with positive magnetostriction have been isochronally irradiated with a pulsed excimer laser using different repetition rates and pulse energies. Laser-treatment-induced effects on the magnetic properties and amorphous nature of metallic glasses have been studied by transmission Mössbauer spectroscopy (TMS) and conversion electron Mössbauer spectroscopy (CEMS). Related morphologi-

cal changes have been examined by scanning electron microscopy (SEM), and the resultant crystalline precipitates were characterized by energy-dispersive x-ray analysis (EDX). The laser-induced changes in the magnetic anisotropy were found to depend on the values of the irradiation parameters and magnetostriction constants.

These results are consistent with the formation of a closure domain structure due to magnetoelastic interactions in ferromagnetic amorphous ribbons. The effect of excimer-laser-induced crystallization is reported in metallic glasses using high values of the repetition rate and pulse energy. The first crystalline phase to appear has been identified. The observed phase transformation can be explained by employing melt model calculations of high-fluence laser irradiation.

II. EXPERIMENTAL PROCEDURES

A. Laser processing

Amorphous alloys $\text{Fe}_{66}\text{Co}_{18}\text{B}_{15}\text{Si}_1$ (Metglas 2605 CO), $\text{Fe}_{74}\text{Ni}_4\text{Mo}_3\text{B}_{17}\text{Si}_2$ (Metglas 2605 SM), $\text{Fe}_{40}\text{Ni}_{38}\text{Mo}_4\text{B}_{18}$ (Metglas 2826 MB), and $\text{Fe}_{77}\text{Cr}_2\text{B}_{16}\text{Si}_5$ (Metglas 2605-S3A), selected with respect to the different values of their magnetostriction constants, were supplied by Allied Signal Inc. in the form of 25- μm thick ribbons. Square samples (2 \times 2 cm) were cut from the foils and exposed on the shiny side to the $\lambda=308$ nm radiation generated by a XeCl excimer laser (Lambda Physik), having the pulse width at half maxima $\tau=26$ ns. Pulse energies of 50 and 75 mJ/pulse were employed. Single-pulse energy densities of 20–30 mJ/mm² were achieved by focusing with a cylindrical fused silica lens to a spot size of about 0.5 \times 5 mm². Recent irradiation experiments¹⁰ performed on $\text{Fe}_{80}\text{B}_{20}$ samples ($\lambda=308$ nm, $\tau=20$ ns, $w=20$ mJ/mm²)

irradiated with five laser pulses per spot at repetition rates of 1 and 10 Hz have shown that excimer-laser-irradiation effects in metallic glasses depend strongly on the values of the repetition rate employed. In the present paper, the amorphous samples were isochronally irradiated for $t=5$ s per spot, using repetition rates which ranged from 1–50 Hz. An acceptable degree of irradiation homogeneity (as checked by SEM) was obtained by laser beam scanning of the whole sample surface, which was placed on an x - y - z micrometer translation stage.

B. Experimental techniques

Room-temperature transmission Mössbauer measurements were made with a constant acceleration spectrometer (Ranger Scientific). The ~ 25 mCi γ -ray source was ^{57}Co in a Rh matrix, maintained at room temperature. Automatic laser velocity calibration with a digital feedback system was used. TMS spectra of as-received and laser-irradiated samples were collected with incident γ rays perpendicular to the ribbon plane. Amorphous specimen spectra were analyzed with a least-squares program¹² by constraining the relative areas of the outer:inner line pairs to the ratio 3:1.

CEMS spectra of as-cast and laser treated surfaces of the metallic samples were collected using a flowing He-CH₄ electron counter.¹³ The back-scattered electrons into 2π solid angle were recorded, so that the behavior of surface layers of ~ 100 nm could be detailed.

SEM investigations were performed without further surface preparation using a Jeol electron microscope at 25 keV, operating in the secondary-electron-emission mode. Chemical analysis of select microvolumes in the partially crystallized sample was carried out with a Tracor Northern EDX spectrometer.

III. RESULTS AND DISCUSSION

A. Induced magnetic anisotropy in metallic glasses by pulsed-excimer-laser irradiation

Room-temperature transmission Mössbauer spectra of the Metglas 2605 CO, 2605 SM, and 2826 MB samples in the amorphous as-quenched state are shown in Figs. 1(a), 2(a), and 3(a), respectively. For the 14.4-keV γ rays of ^{57}Fe , the relative intensity of the second (fifth) to the first (sixth) lines is given, in the thin absorber approximation, by¹⁴ $R_{21}=4 \sin^2\alpha/3(1+\cos^2\alpha)$, where α is the angle between the γ -ray propagation direction and the direction of the magnetic hyperfine moment. The ratio R_{21} varies from 0 to $\frac{4}{3}$ as α changes from 0° to 90° and for a completely random distribution of magnetic-moment directions, takes the value 0.67. Consequently, the calculated values of the areal ratio ($R_{21}=1.04$, 1.14, and 1.09, respectively) show that the magnetic moments of the as-prepared materials are preferentially oriented in the plane of the ribbons, as observed for other amorphous alloys with similar compositions.^{15–17}

It can be seen in Fig. 1(b), for the 2605 CO sample irradiated with 50 mJ/pulse at the repetition rate of 1 Hz, that the laser-induced effects have resulted in a pro-

nounced decrease of the intensity ratio of the second to the first line. The corresponding value $R_{21}=0.19$ shows that a rotation of the average magnetic-moment directions from the in-plane ($\alpha=90^\circ$) to an out-of-plane orientation has taken place. For the 2605 CO samples irradiated at repetition rates of 10, 25, and 35 Hz [Figs. 1(c)–1(e), respectively], the relative intensity of lines R_{21} progressively increases as compared to the spectrum in Fig. 1(b), but the corresponding values 0.23, 0.29, and 0.36 are still far from the value indicating the random distribution of magnetic-moment directions. Thus, the average magnetic-moment direction for the 2605 CO samples has been observed to maintain a preferred out-of-plane orientation upon laser annealing.

Figures 2(b)–2(e) show the Mössbauer spectra taken at room temperature for the 2605 SM samples, after isochronal excimer-laser irradiation using repetition rates in the range 1–35 Hz. The fitted values of the areal ratio ($R_{21}=0.20$, 0.26, 0.34, and 0.50, respectively) indicate a similar reorientation of the bulk magnetization direction, as a consequence of the laser treatment performed. However, the induced easy magnetization axis lies closer to the plane of the foil, compared to the laser-irradiated 2605 CO samples. This result can be assigned to the fact that the magnetostriction constant ($\lambda_s=19$ ppm) of the 2605 SM amorphous alloy has a lower value than that of the 2605 CO ($\lambda_s=35$ ppm) metallic glass. Indeed, it is known from previously reported annealing studies^{9,18} that the induced anisotropy energy is greater in the higher magnetostriction samples than in the lower λ_s ones. These results show that it is possible to induce controlled changes in the direction of bulk magnetization in higher magnetostriction samples, through the appropriate selection of irradiation parameters.

Room-temperature Mössbauer spectra of the 2826 MB samples, after irradiation with the same parameter values used for previously studied iron-based amorphous alloys are presented in Figs. 3(b)–3(d). The refined values of the intensity ratio of the second and fifth to the outermost lines ($R_{21}=0.43$, 0.45, and 0.57, respectively) show that the pulsed laser treatment performed has also induced a reorientation of the magnetic-moment directions in this nickel–iron-based amorphous alloy. However, the easy magnetization axis is considerably closer to the ribbon plane, in comparison with the laser-irradiated iron-based metallic glasses. This result can be attributed to the fact that the magnetostriction constant of the 2826 MB nickel–iron-based alloy ($\lambda_s=12$ ppm) has a significantly lower value than that of the iron-based metallic glasses. Moreover, after isochronal irradiation with 50 mJ/pulse at the repetition rate of 35 Hz [Fig. 3(e)], the random distribution of magnetic-moment directions was achieved ($R_{21}=0.66$), indicating a relief of the induced stresses, as compared to the spectrum in Fig. 3(b). One may note that the occurrence of two opposite effects was observed in cw laser annealing as well: relaxation of stresses and/or production of stresses.¹⁹

The intensity ratio R_{21} is represented in Fig. 4(a) as a function of the repetition rate between the laser pulses for all compositions studied. By monitoring the kinetics of transverse induced magnetic anisotropy in the irradiated

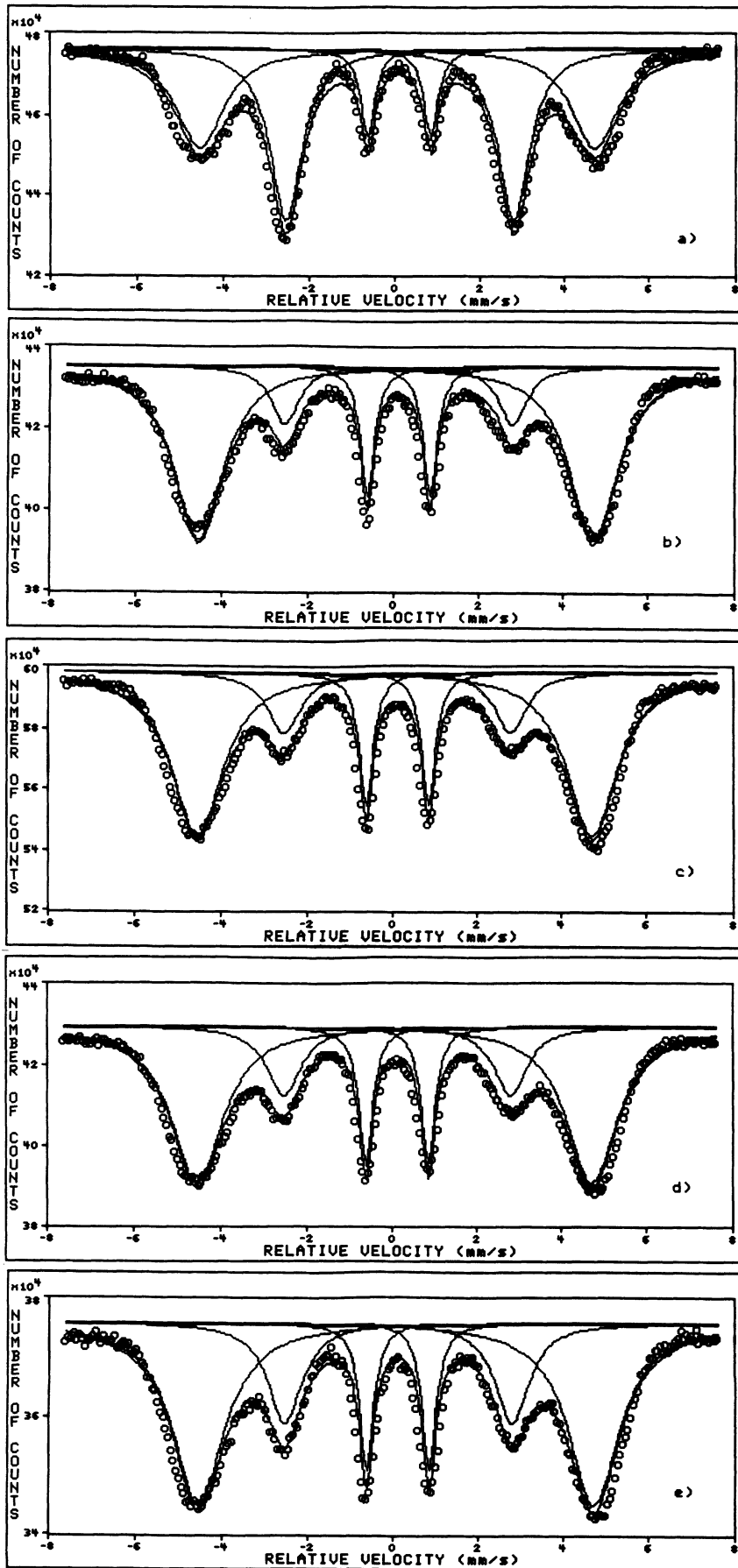


FIG. 1. Room-temperature transmission Mössbauer spectra of Metglas 2605 CO samples: (a) in the amorphous as-quenched state and after pulsed-excimer-laser irradiation ($\lambda=308$ nm, $\tau=26$ ns, $E=50$ mJ/pulse, $t=5$ s) at repetition rates of: (b) 1 Hz; (c) 10 Hz; (d) 25 Hz; (e) 35 Hz. Velocity scale is calibrated relative to α -Fe at 300 K.

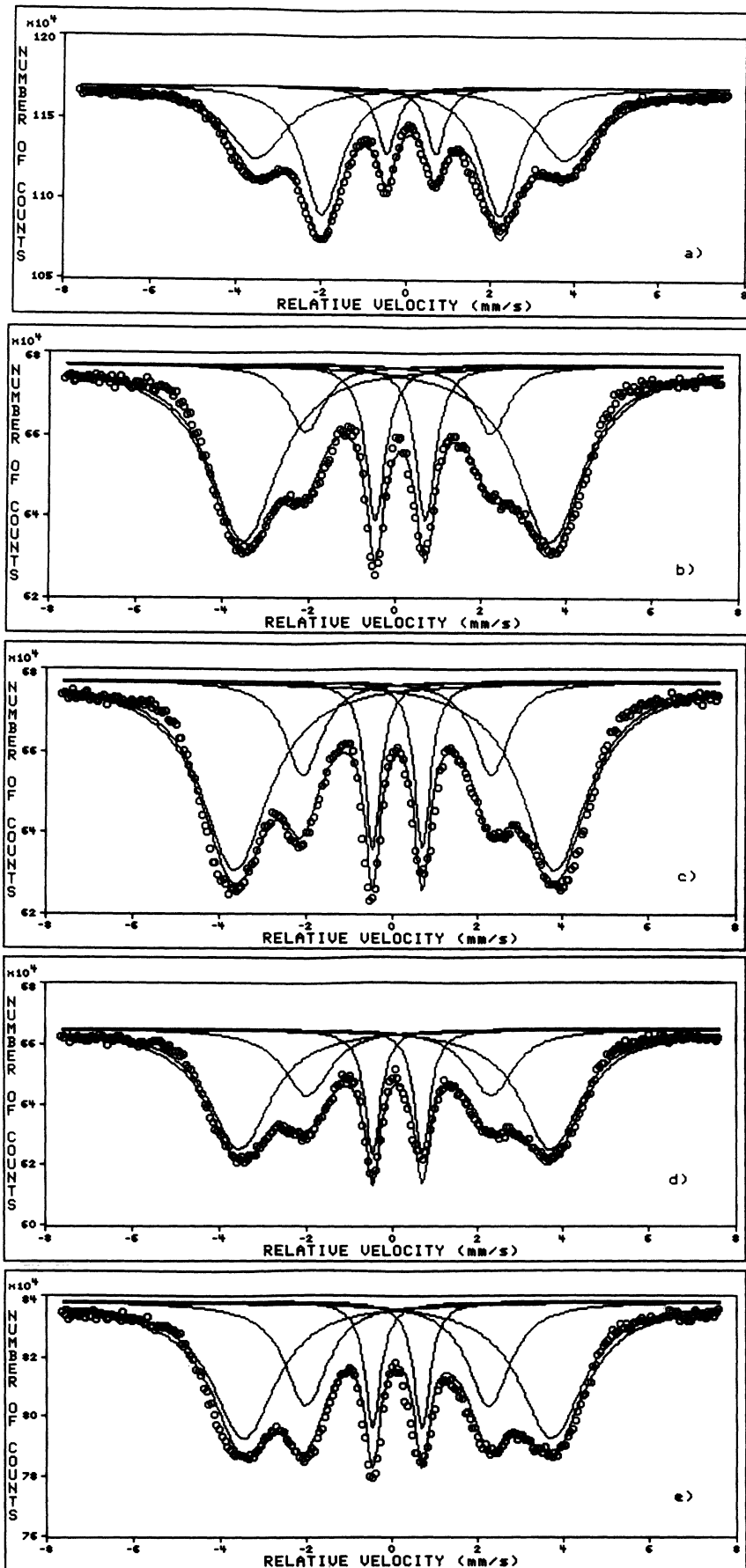


FIG. 2. Room-temperature TMS spectra of Metglas 2605 SM samples: (a) in the amorphous as-quenched state and after pulsed-excimer-laser irradiation for 5 s at 50 mJ/pulse and repetition rates of: (b) 1 Hz; (c) 10 Hz; (d) 25 Hz; (e) 35 Hz.

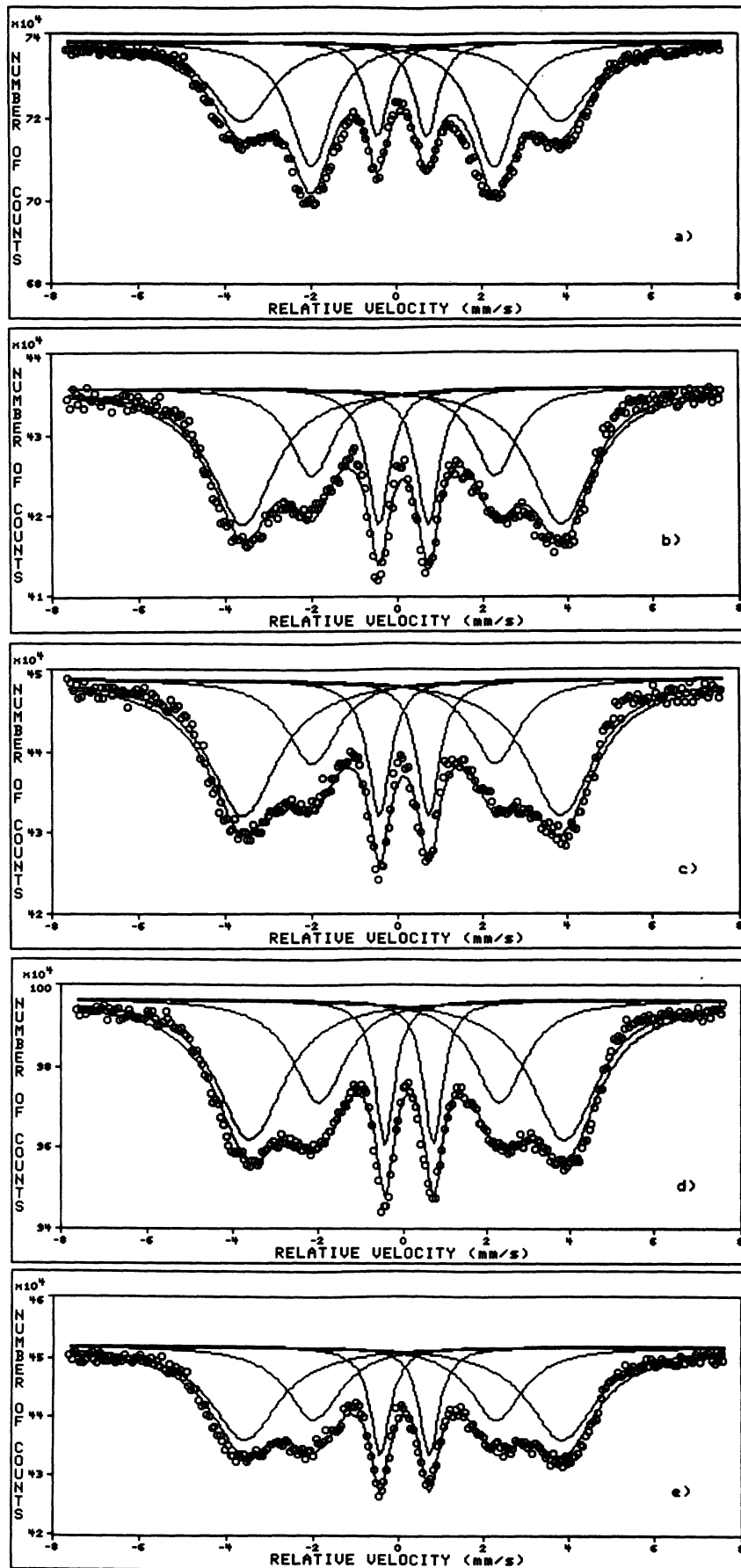


FIG. 3. Room-temperature TMS spectra of Metglas 2826 MB samples: (a) in the amorphous as-quenched state and after pulsed-excimer-laser irradiation for 5 s at 50 mJ/pulse and repetition rates of: (b) 1 Hz; (c) 10 Hz; (d) 25 Hz; (e) 35 Hz.

amorphous systems, these plots show that in higher magnetostriction, iron-based metallic glasses, controlled magnetic anisotropy is obtained as an effect of isochronal excimer-laser irradiation, whereas in the low magnetostriction nickel-iron-based alloy samples, the random distribution of magnetic moments can be achieved. The role played by the values of the magnetostriction constant in explaining the magnitude of induced anisotropies is outlined by the fact that all amorphous systems considered in this study have identical values of tensile strength and elastic modulus.²⁰ Consequently, the magnetic anisotropy induced by the laser treatment performed is directly dependent on the values of the magnetostriction constants. This is a result which could not be

obtained for samples with positive magnetostriction constants by local laser annealing,⁵ due to the opposing effects of magnetoelastic and magnetostatic interactions in inhomogeneously irradiated samples.

In order to explain a similar development of transverse magnetic anisotropy in thermal annealing treatments, the model of closure domain structure has been proposed.^{21,22} It relies on the development of tensile stresses in the surface and compressive stresses in the bulk, due to the formation of surface crystalline phases of higher density. Thus, in specimens with positive magnetostriction,

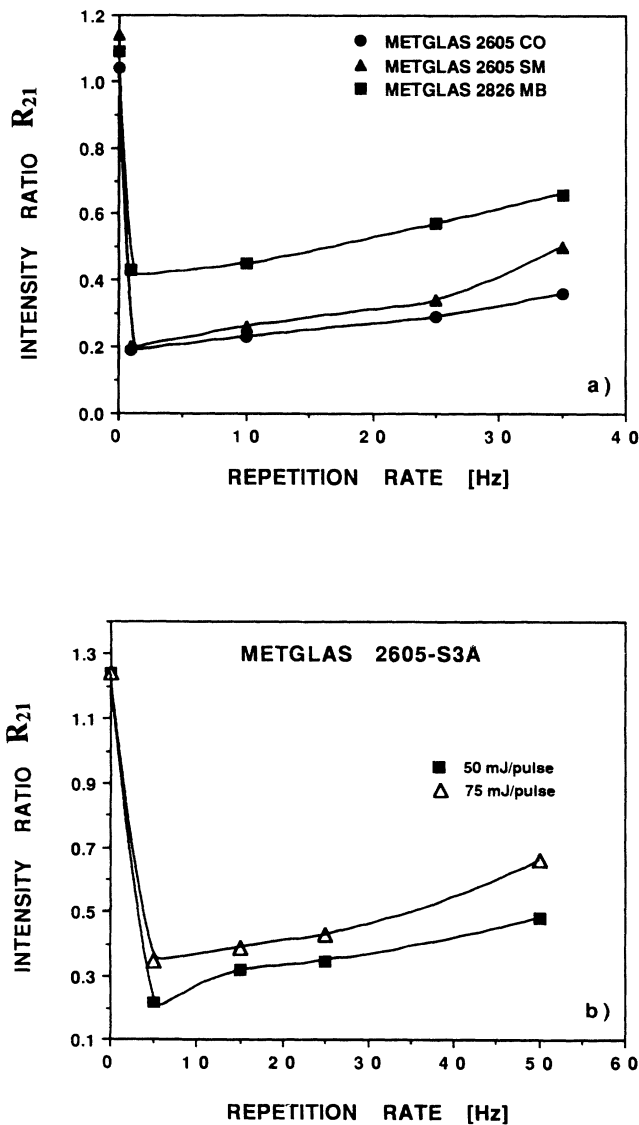


FIG. 4. Relative intensity of the second to the first line of the transmission Mössbauer spectra as a function of the repetition rate between the laser pulses: (a) for Metglas 2605 CO, 2605 SM, and 2826 MB samples at 50 mJ/pulse and (b) for Metglas 2605-S3A samples at 50 and 75 mJ/pulse. The solid lines are drawn as guides for the eye and the error bars are included in the data symbols.

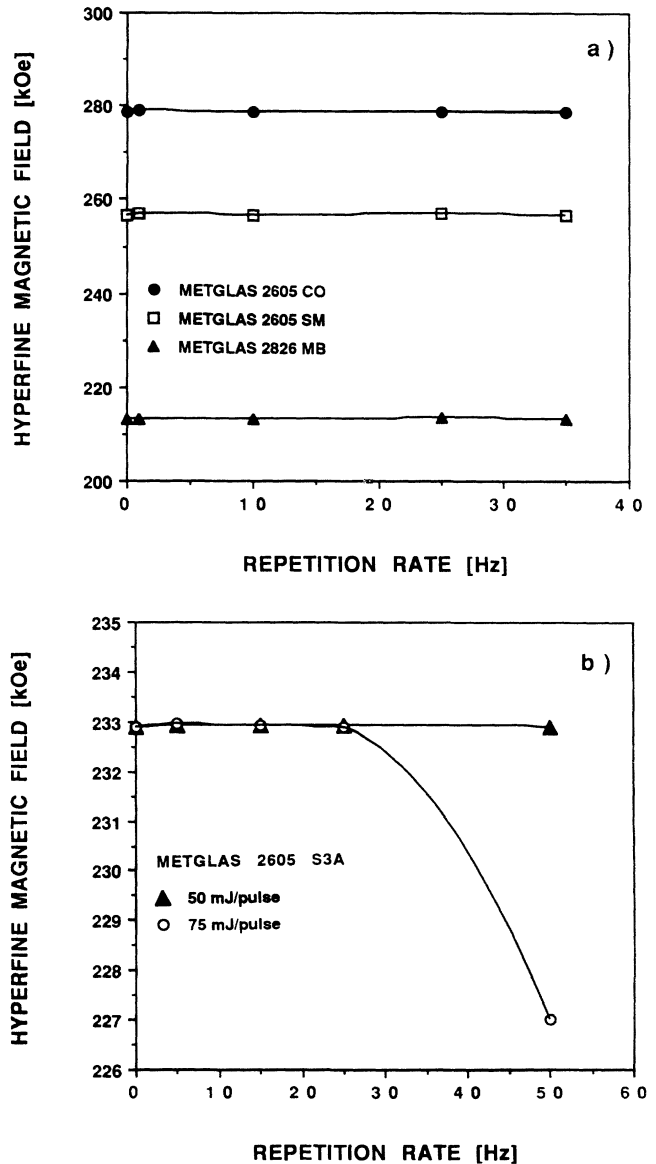


FIG. 5. Hyperfine magnetic field of amorphous component as a function of the repetition rate employed in excimer-laser irradiation: (a) for Metglas 2605 CO, 2605 SM and 2826 MB samples at 50 mJ/pulse and (b) for Metglas 2605-S3A samples at 50 and 75 mJ/pulse. The pulse energies correspond to approximate fluence values of 20 and 30 mJ/mm², respectively. The solid lines are drawn as guides for the eye and the errors are considered in the size of the data markers.

these stresses cause atomic spins to rotate in a direction out of the ribbon plane. This model can also explain the magnetic anisotropy induced in the present irradiation study, after properly identifying the surface modifications which may have caused the dramatic changes of bulk magnetic properties.

As can be inferred from Fig. 5(a), the laser treatment performed had no significant effect on the values of the hyperfine magnetic fields in any of the amorphous compositions studied. Consequently, our bulk Mössbauer experiments reveal no crystalline phases in either iron-based or nickel-iron-based alloy samples, indicating that excimer-laser irradiation of metallic glasses does not cause the onset of bulk crystallization^{7,9} when moderate values of the repetition rate and pulse energy are used.

Selected conversion electron Mössbauer spectra of the as-quenched and pulsed laser-irradiated samples are shown in Figs. 6(a) and 6(b). For all compositions studied and irradiation parameters employed, the CEMS spectra of the irradiated surfaces were characteristic of the amorphous state, reflecting the absence of crystalline phases within the 100-nm thick surface layers. The CEMS spec-

tra of the laser treated sides, however, showed the same magnetic texture as the nonirradiated surfaces, in contrast to the textural changes observed for the bulk sample measurements. These results show that a thin surface layer of the irradiated foils preserves the in-plane domain structure of the untreated samples, suggesting the existence of a distribution of magnetic-moment directions through the thickness of the foils.^{7,10} Consequently, the CEMS measurements reject surface crystallization as a possible cause of compressive stress formation. In order to investigate the surface morphological modifications which may have caused the observed changes in the easy magnetization axis, SEM examinations of the laser-irradiated surfaces have also been performed [Figs. 7(a)–7(c)]. They reveal the presence of molten zones, which were subsequently resolidified, and of correspondingly induced complex mechanical stresses. Similarly, the changes in the bulk properties of laser treated Pd-Si glasses have been attributed to the effect of laser-induced shock waves.^{23,24} These result in boiling of the metal surface and plasma production, due to a dramatic increase in the surface temperature and a simultaneous decrease in

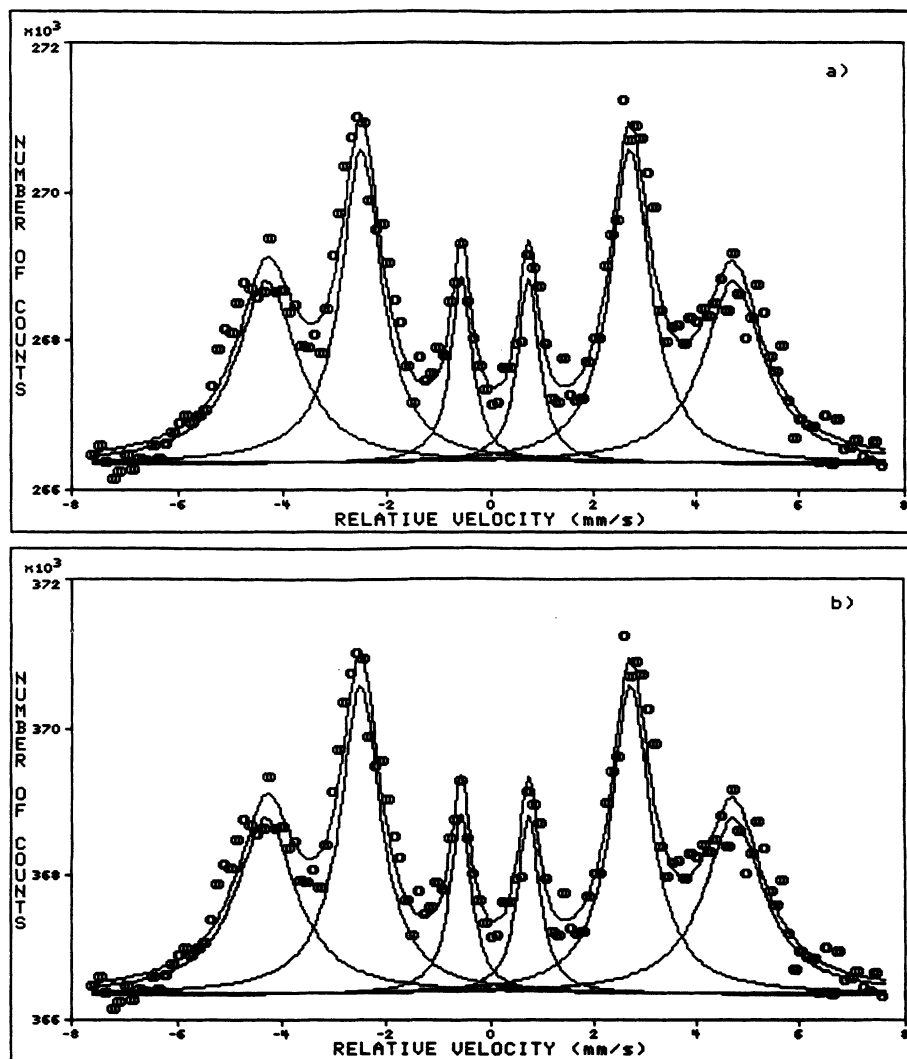


FIG. 6. CEMS spectra of the Metglas 2605 CO samples: (a) in the amorphous as-quenched state and (b) after pulsed-excimer-laser irradiation for 5 s at 50 mJ/pulse and a repetition rate of 35 Hz.

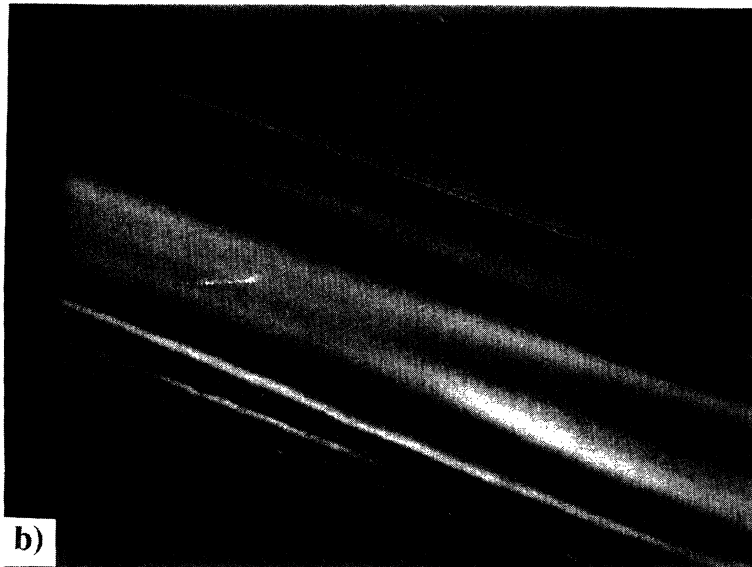
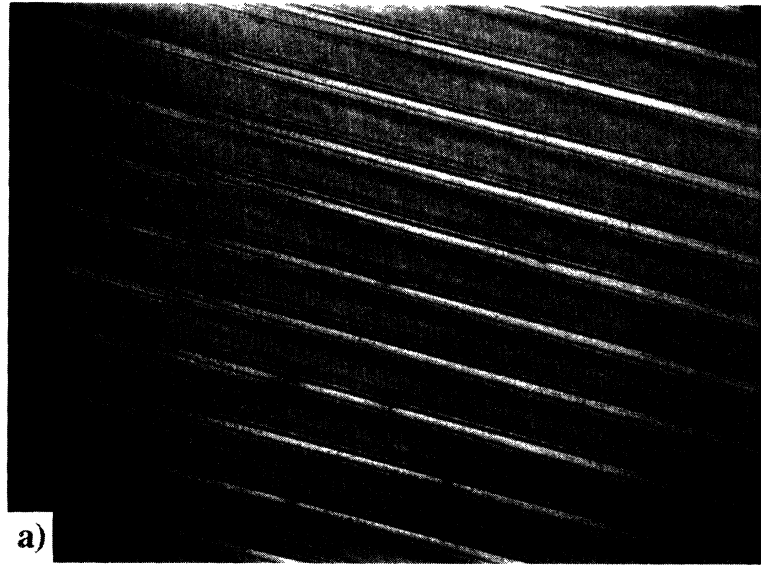


FIG. 7. SEM examinations of the Metglas 2605 SM samples, after excimer-laser irradiation for 5 s at 50 mJ/pulse and a repetition rate of 35 Mz; the magnification employed had the values: (a) $\times 18$; (b) $\times 200$; (c) $\times 4800$.

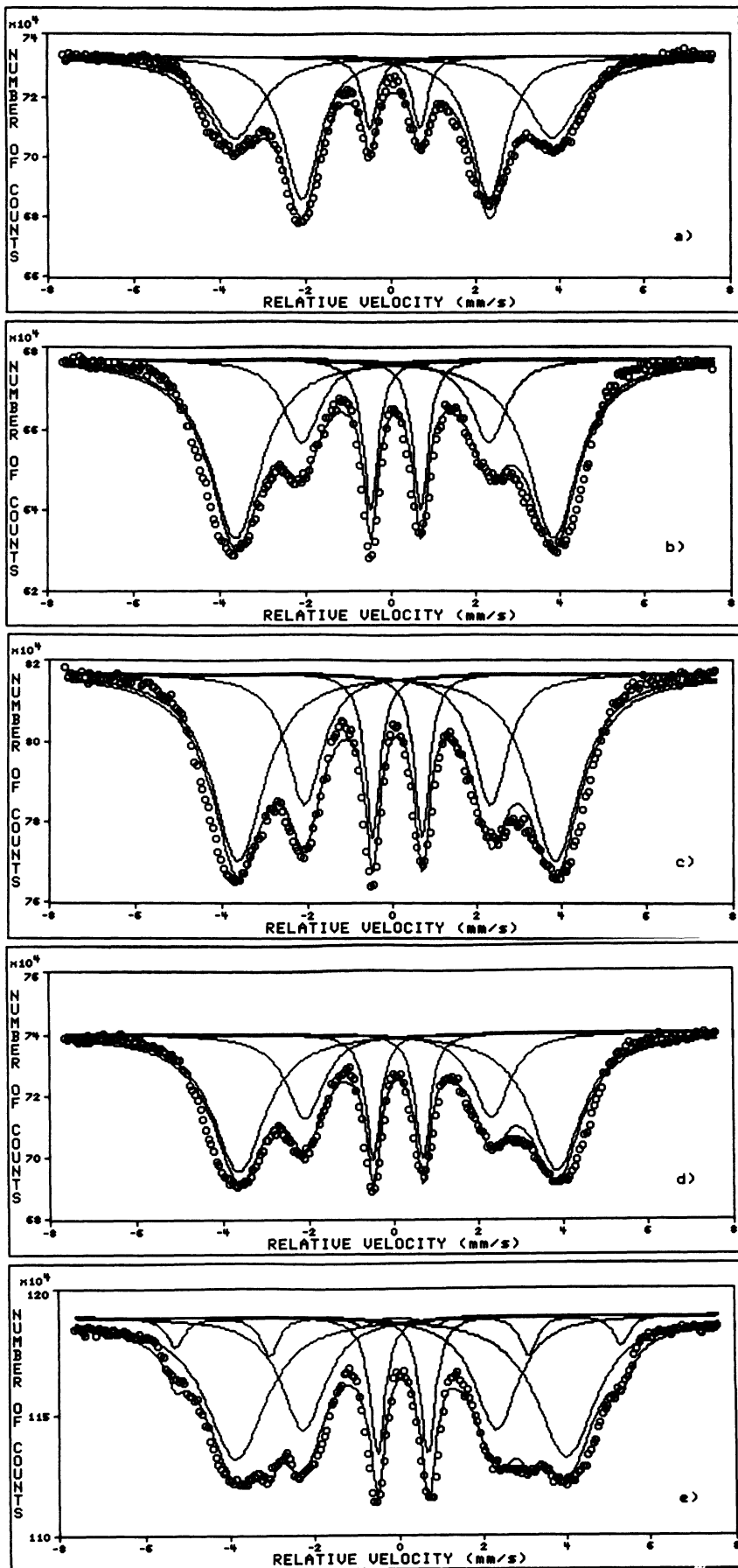


FIG. 8. Room-temperature TMS spectra of the Metglas 2605-S3A samples: (a) in the amorphous as-quenched state and after pulsed-excimer-laser irradiation ($\lambda=308$ nm, $\tau=26$ ns, $t=5$ s) with (b) 50 mJ/pulse at a repetition rate of 25 Hz, (c) 50 mJ/pulse at a repetition rate of 50 Hz, (d) 75 mJ/pulse at a repetition rate of 25 Hz, (e) 75 mJ/pulse a repetition rate of 50 Hz.

the metal's reflectivity. Related ablation pressures are high enough to change interatomic distances and cause atomic rearrangements or homogenization of the amorphous phase.⁴ It follows that the corresponding in-plane compressive stresses have caused the atomic spins to rotate in a direction normal to the sample surface. Consequently, the in-plane domain structure of the nonirradiated foils was changed by the laser treatment, due to magnetoelastic effects, to a closure domain structure.^{7,10,21,22}

B. Induced phase transformation in metallic glasses by pulsed-excimer-laser irradiation

The results presented in this section concern the amorphous ferromagnetic alloy, $\text{Fe}_{77}\text{Cr}_2\text{B}_{16}\text{Si}_5$ (Metglas 2605-S3A). This material has a Curie temperature of 622 K, a crystallization temperature of 809 K, and a magnetostriction constant of 20 ppm.^{20,25} Selected room-temperature transmission Mössbauer spectra of the as-quenched and isochronal excimer-laser-irradiated 2605-S3A samples are presented in Figs. 8(a)–8(e). The intensity ratio R_{21} derived from the TMS spectra is plotted in Fig. 4(b) as a function of the repetition rate between the applied laser pulses for both values of the pulse energy employed. These plots show that the effects of pulsed-excimer-laser irradiation on the magnetic anisotropy of the amorphous alloy samples depend both on the repetition rate and pulse energy. At moderate values of the repetition rate and pulse energy, controlled changes in the direction of bulk magnetization can be obtained through a suitable choice of irradiation parameters; at higher values of the repetition rate and pulse energy, the random distribution of magnetic-moment directions has resulted. This behavior is in good agreement with the dependence of the intensity ratio of the second to the first line, as determined by isochronal excimer-laser annealing of the iron-based and nickel-iron-based alloy samples studied in Sec. III A.

When a high-fluence irradiation treatment was performed (75 mJ/pulse at the repetition rate of 50 Hz), however, the excimer-laser-induced effects were found to affect the amorphous nature of the irradiated sample. The corresponding transmission Mössbauer spectrum [Fig. 8(e)] reveals the presence of an additional six-line pattern characteristic of a crystalline phase, with the hyperfine parameters corresponding to α -Fe. Indeed, α -Fe was found to be the first crystalline phase to precipitate out in several previous thermal^{26–30} and radio-frequency³¹ annealing studies of Fe-B alloys with <17% boron content. The relative areas of component patterns in the transmission Mössbauer spectrum indicate a composition of 9% α -Fe in a metalloid-enriched amorphous matrix. The corresponding decrease of the internal magnetic field of the amorphous component (from 232.9 to 227 kOe) supports the onset of bulk crystallization by α -Fe precipitation [Fig. 5(b)]. In addition, it should be mentioned that the transmission Mössbauer spectrum analysis indicated a 3:4:1:1:4:3 relative line intensity in the α -Fe sextet, showing that the magnetic moments of the first crystalline phase formed were preferentially

oriented in the plane of the irradiated foil. Consequently, the TMS results support the onset of excimer-laser-induced crystallization, observed in amorphous alloys in the present study by the precipitation of a textured form of the most abundant constituent element.

It can be seen by examination of Fig. 9(a), that the SEM investigations reveal the presence of micron-size islands of iron-rich precipitates and seem to indicate a greater oxidation of iron in the excimer-laser-irradiated $\text{Fe}_{77}\text{Cr}_2\text{B}_{16}\text{Si}_5$ sample. One may note that a higher degree of oxidation of both boron and iron was observed in $\text{Fe}_{80}\text{B}_{20}$ after picosecond laser treatment⁴ and in $\text{Fe}_{81}\text{B}_{13.5}\text{Si}_{3.5}\text{C}_2$ after isochronal pulsed-radio-frequency annealing.^{32,33}

In order to gain additional information regarding the nature of the crystalline precipitates observed in the present irradiation study, EDX analysis of the corresponding microvolumes has also been performed [Fig. 9(b)], as this technique is known to provide an average chemical composition over a volume of a cubic micron.³⁴ On these grounds, the α -Fe precipitates were found to contain an extremely low amount ($\sim 0.2\%$) of chromium atoms, which could not be evidenced by bulk Mössbauer measurements. These results tend to support the identification of the α -Fe(Cr) phase as the first crystalline product in $\text{Fe}_{78}\text{B}_{13}\text{Si}_{3.5}\text{Cr}_{5.5}$ and $\text{Fe}_{78}\text{B}_{13}\text{Si}_{2.5}\text{Cr}_{6.5}$ amorphous alloys.³⁵ However, our EDX technique is not sensitive to chemical elements with atomic number $Z < 11$, so that the presence of oxygen or boron could not be determined using this method.³⁴ Instead, CEMS spectra were previously found to provide information on the presence of iron oxide particles, even when transmission Mössbauer spectra failed to identify them.^{32,36}

The conversion electron Mössbauer spectrum recorded on the shiny (irradiated) side of the 2605-S3A sample, after the high-fluence pulsed-excimer-laser irradiation (75 mJ/pulse, 50 Hz) is given in Fig. 10. CEMS spectrum analysis indicates the presence of the six-line pattern corresponding to the textured α -Fe(Cr) crystalline phase, the broadened sextet associated with the remaining iron-depleted amorphous matrix, and an additional quadrupole-split doublet (quadrupole splitting 0.78 mm/s, isomer shift 0.15 mm/s), which is likely to correspond to nonstoichiometric iron oxides.^{32,36} Indeed, one is tempted to assume an oxidation mechanism of Fe^0 to Fe^{2+} , which initially leads to the precipitation of FeO islands,³⁶ a mechanism which could explain the oxidation effects previously observed in isochronal pulsed-radio-frequency annealing of some Fe-B metallic glasses.^{32,33} The relative composition of the upper 100 nm layer, as obtained from the present CEMS investigations of the laser-irradiated surface, corresponds to 7% α -Fe(Cr) and 32% iron oxides; the balance of the composition is represented by the remaining amorphous component. Consequently, through combined application of several complementary methods of investigation, the nature of the phase transformation observed in $\text{Fe}_{77}\text{Cr}_2\text{B}_{16}\text{Si}_5$ metallic glass after high-fluence excimer-laser irradiation has been elucidated and found to consist of partial crystallization and surface oxidation of the amorphous material. As the oxide layer is easily removed by conven-

tional methods,^{33,37} partial crystallization of metallic glasses may be of interest in applications such as delay lines and stress sensors,³ in order to induce transverse anisotropies and/or to modulate the magnetoelastic properties for the specific applications.

To our knowledge, a theoretical model that would explain both thermal and stress-related effects in laser-irradiated metallic glasses is not available, since it would require knowledge of the temperature dependence of thermal and optical properties of the material under study. However, melt model calculations developed for excimer-laser irradiation of silicon can be used to obtain order-of-magnitude predictions regarding the kinetics of laser-induced melting in highly absorbing materials. In this model, the depth of the molten layer (d) formed dur-

ing an intense laser pulse of duration τ is $d = (2D\tau)^{1/2}$, where $D = \kappa/C_v\rho$ is the heat diffusivity of the material with thermal conductivity κ , specific heat C_v , and density ρ . For a typical D value for metals³⁸ of $D \sim 0.5 \text{ cm}^2/\text{s}$, d is found to be $\sim 1.5 \mu\text{m}$ for 26 ns laser pulses. Considering the experimental data available for silicon irradiated with 20 ns pulses of $30 \text{ mJ}/\text{mm}^2$ excimer-laser fluences,³⁹ a lifetime of the molten layer (t_m) of 150 ns is obtained. Assuming a similar behavior of metals and a diffusivity in the liquid phase $D_l \sim 10^{-4} \text{ cm}^2/\text{s}$, the mixing length $\lambda = (D_l t_m)^{1/2}$ is found to be $\sim 40 \text{ nm}$. This mixing length value defines an upper limit for the influence of nanosecond laser irradiation on the surface inhomogeneities and is known to be significantly higher than the

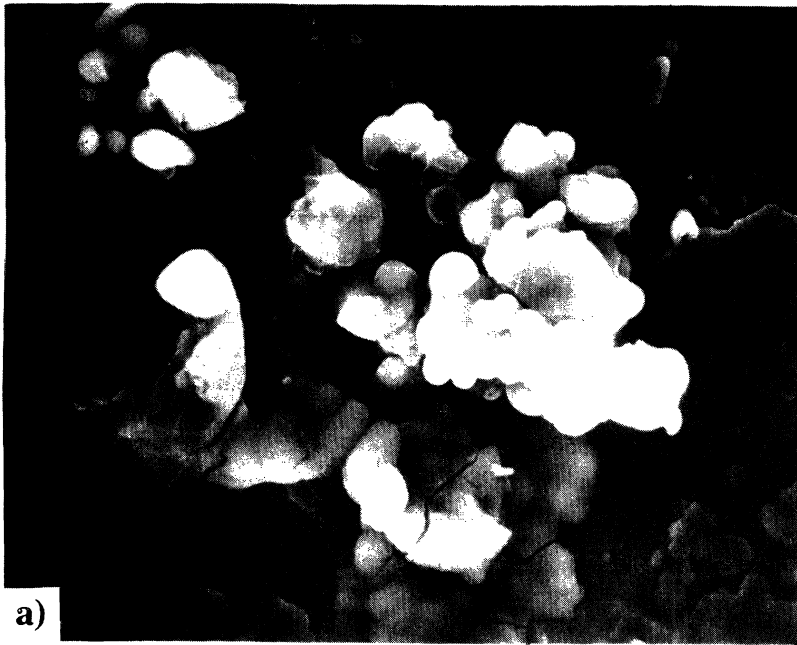
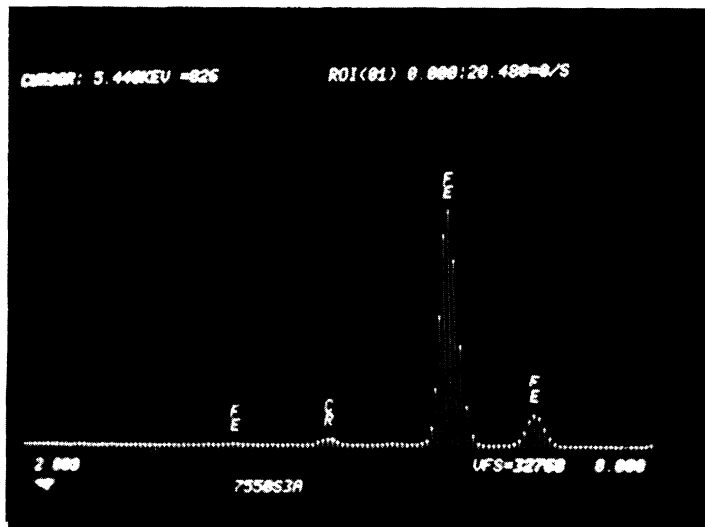


FIG. 9. (a) SEM photograph ($\times 2000$) and (b) EDX examination of the Metglas 2605-S3A sample irradiated with $75 \text{ mJ}/\text{pulse}$ at a repetition rate of 50 Hz.



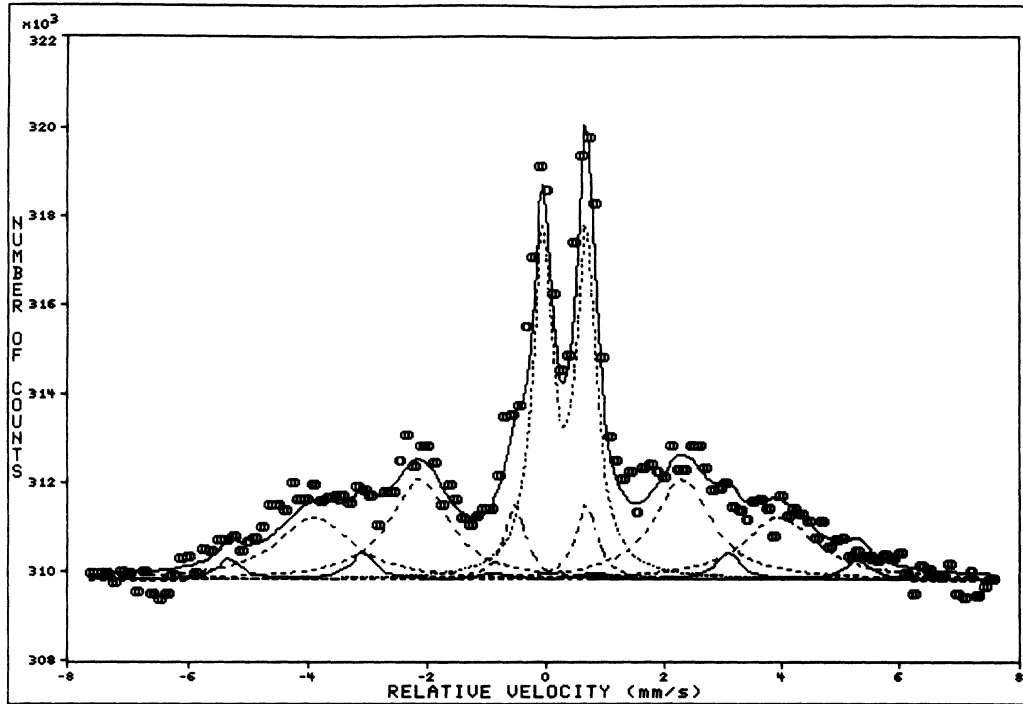


FIG. 10. CEMS spectrum of the Metglas 2605-S3A sample, recorded on the shiny side after pulsed-excimer-laser irradiation for 5 s at 75 mJ/pulse and a repetition rate of 50 Hz.

critical radius of crystallization nuclei at room temperature.^{4,40} On these grounds, one can infer that the use of high fluences results in melting to a sufficient depth for the thermal energy stored in the liquid layer to prolong the duration of melting; cooling and solidification then occurs slowly enough so that crystalline growth results. Consequently, the present study demonstrates the existence of a window of energy density, within which amorphous phase formation is favored after pulsed-excimer-laser irradiation of metallic glasses. The laser treatment proposed in the present work can be used to induce different anisotropies or partial crystallization in amorphous alloys, through the appropriate selection of irradiation parameters.

IV. CONCLUSIONS

The main results obtained in the present study can be summarized as follows.

(i) The effects of pulsed-excimer-laser irradiation on the magnetic anisotropy of iron-rich metallic glasses depend on the values of the irradiation parameters (pulse energy, number of applied laser pulses per spot, and repetition rate) and on the material properties (magnetostriction constants). The presence of laser molten zones subsequently quenched and of related mechanical stresses sup-

ports the model of closure domain structure.

(ii) Pulsed-excimer-laser irradiation at high repetition rates and pulse energies is found to affect both the magnetic anisotropy and the amorphous nature of metallic glasses. Laser-induced phase transformation in Metglas 2605-S3A was investigated by complementary methods and found to consist of partial crystallization and surface oxidation. The bulk and surface crystalline products were identified and their relative composition, magnetic texture, and morphology were studied. The effect of excimer-laser-induced crystallization in metallic glasses, observed in the present study, was explained by consideration of melt model calculations for high-fluence laser irradiation.

(iii) Through an adequate selection of irradiation parameters, the effects of induced anisotropy and partial crystallization can be used following the laser treatment proposed for modulating the magnetoelastic properties of amorphous metals with respect to specific applications.

ACKNOWLEDGMENTS

This work has been supported by the National Science Foundation and the Office of Naval Research.

¹A. Slawska-Waniewska, A. Siemko, J. Finck-Finowicki, L. Zaluski, and H. K. Lachowicz, *J. Magn. Magn. Mater.* **101**, 40 (1991).

²J. Gonzalez and J. M. Blanco, *J. Non-Cryst. Solids* **126**, 151

(1990).

³P. Matteazzi, L. Lanotte, and V. Tagliaferri, *Hyperfine Interact.* **45**, 315 (1989).

⁴A. P. Radlinski, A. Calka, and B. Luther-Davies, *Mater. Sci.*

- Eng. **97**, 253 (1988).
- ⁵C. Aroca, M. C. Sanchez, I. Tanarro, P. Sanchez, E. Lopez, and M. Vazquez, *Phys. Rev. B* **42**, 8086 (1990).
- ⁶R. T. Young and R. F. Wood, in *Semiconductors and Semimetals*, edited by R. F. Wood, C. W. White, and R. T. Young (Academic, Orlando, 1984), Vol. 23, p. 626.
- ⁷P. Schaaf, A. Kramer, L. Blaes, G. Wagner, F. Aubertin, and U. Gonser, *Nucl. Instrum. Methods* **53**, 184 (1991).
- ⁸D. Sorescu, M. Sorescu, A. Hening, I. N. Mihailescu, and D. Barb, *Rom. Rep. Phys.* **44**, 787 (1992).
- ⁹D. Sorescu, M. Sorescu, I. N. Mihailescu, D. Barb, and A. Hening, *Solid State Commun.* **85**, 717 (1993).
- ¹⁰M. Sorescu, E. T. Knobbe, D. Barb, D. Sorescu, and I. Bibicu, *Hyperfine Interact.* (to be published).
- ¹¹M. Sorescu and E. T. Knobbe, *J. Mater. Res.* **8**, 3078 (1993).
- ¹²F. D. Barb, O. Netoiu, M. Sorescu, and M. Weiss, *Comput. Phys. Commun.* **69**, 182 (1992).
- ¹³J. J. Spijkermaan, in *Mössbauer Effect Methodology*, edited by I. J. Gruverman (Plenum, New York, 1971), Vol. 7, p. 85.
- ¹⁴T. E. Cranshaw and G. Longworth, in *Mössbauer Spectroscopy Applied to Inorganic Chemistry*, edited by G. J. Long (Plenum, New York, 1984), Vol. 1, p. 173.
- ¹⁵J. Sitek, M. Miglierini, J. Lipka, P. Valko, and I. Toth, *Hyperfine Interact.* **60**, 777 (1990).
- ¹⁶I. Skorvanek, A. Zentko, M. Miglierini, and J. Kovac, *Hyperfine Interact.* **59**, 301 (1990).
- ¹⁷P. J. Schurer and A. H. Morrish, *J. Magn. Magn. Mater.* **15-18**, 577 (1980).
- ¹⁸P. Sanchez, M. C. Sanchez, E. Lopez, M. Garcia, and C. Aroca, *J. Phys. (Paris)* **12**, 49 (1988).
- ¹⁹L. Lanotte, P. Matteazzi, and V. Tagliaferri, *J. Magn. Magn. Mater.* **42**, 183 (1984).
- ²⁰*Metglas Technical Bulletin* (Allied-Signal, Inc., Parsippany, 1993).
- ²¹H. N. Ok and A. H. Morrish, *Phys. Rev. B* **23**, 2257 (1981).
- ²²N. Saegusa and A. H. Morrish, *Phys. Rev. B* **26**, 305 (1982).
- ²³A. P. Radlinski, A. Calka, and B. Luther-Davies, *Phys. Rev. Lett.* **57**, 3081 (1986).
- ²⁴C. Thomsen, H. T. Grahn, H. J. Maris, and J. Tauc, *Phys. Rev. B* **34**, 4129 (1986).
- ²⁵C. F. Conde, H. Miranda, and A. Conde, *Mater. Lett.* **10**, 501 (1991).
- ²⁶K. Fukamichi, M. Kikuchi, S. Arakawa, and T. Masumoto, *Solid State Commun.* **23**, 955 (1977).
- ²⁷T. Kemeny, I. Vincze, and B. Fogarassy, *Phys. Rev. B* **20**, 476 (1979).
- ²⁸J. C. Swartz, R. Kossowsky, J. J. Haugh, and R. F. Krause, *J. Appl. Phys.* **52**, 3324 (1981).
- ²⁹F. H. Sanchez, M. B. Fernandez van Raap, and J. I. Budnick, *Phys. Rev. B* **46**, 13 881 (1992).
- ³⁰M. Sorescu, S. Stenger, and U. Gonser, *Phys. Status Solidi A* **132**, K57 (1992).
- ³¹S. Stenger, M. Sorescu, and U. Gonser, *J. Non-Cryst. Solids* **151**, 66 (1992).
- ³²M. Rogalski and I. Bibicu, *Mater. Lett.* **13**, 32 (1992).
- ³³M. Rogalski, I. Bibicu, and M. Sorescu, *Hyperfine Interact.* (to be published).
- ³⁴J. B. Wachtman, *Characterization of Materials* (Butterworth-Heinemann and Manning, Stoneham and Greenwich, CT, 1993), Chap. 34.
- ³⁵G. Stergioudis, G. Ivanov, S. C. Chadjivasiliou, A. E. Papadimitriou, C. Achilleos, T. Spassov, I. A. Tsoukalas, *Solid State Commun.* **80**, 89 (1991).
- ³⁶W. Meisel, *J. Phys. (Paris) Colloq. Suppl.* **41**, C1-63 (1980).
- ³⁷A. Gupta, M. E. Jayaraj, S. Lal, and R. P. Verma, *J. Phys. F* **18**, 2159 (1988).
- ³⁸N. Bloembergen, in *Laser Solid Interactions and Laser Processing*, edited by S. D. Ferris, H. J. Leamy, and J. M. Poate (AIP, New York, 1979), Chap. 1.
- ³⁹G. E. Jellison, Jr., D. H. Lowndes, and R. F. Wood, *Proc. SPIE* **710**, 24 (1986).
- ⁴⁰Y. Hirotsu, R. Akada, and A. Onishi, *J. Non-Cryst. Solids* **74**, 97 (1985).

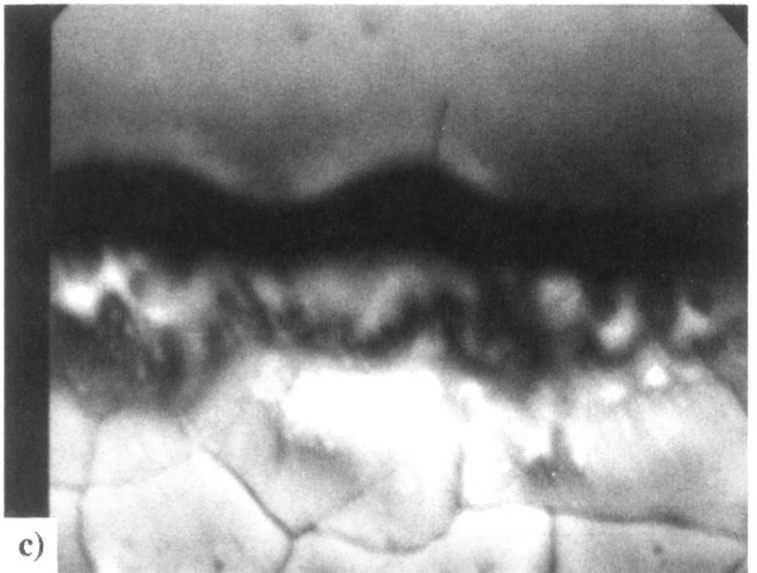
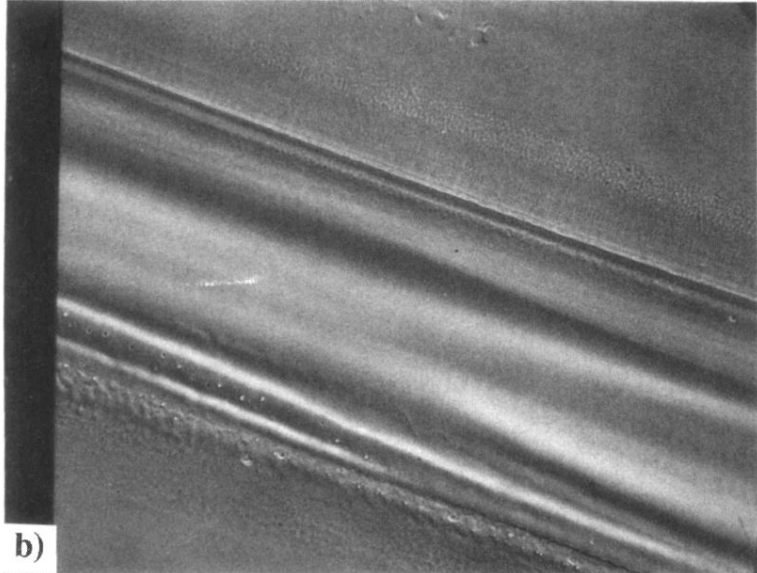
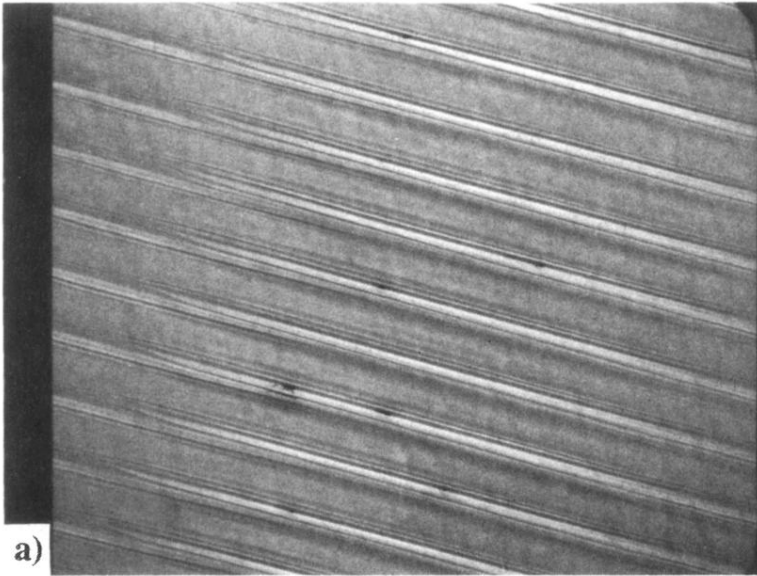


FIG. 7. SEM examinations of the Metglas 2605 SM samples, after excimer-laser irradiation for 5 s at 50 mJ/pulse and a repetition rate of 35 Mz; the magnification employed had the values: (a) $\times 18$; (b) $\times 200$; (c) $\times 4800$.



FIG. 9. (a) SEM photograph ($\times 2000$) and (b) EDX examination of the Metglas 2605-S3A sample irradiated with 75 mJ/pulse at a repetition rate of 50 Hz.

